Experimental Investigation of Velocity and Turbulence Variations in Inclined Jet in Cross-Flow

İbrahim KOÇ[1,*]

[1]*Istanbul Gelisim University, School of Applied Sciences, Department of Aircraft Fuselage-Engine Maintenance, 34310 Avcilar, Istanbul, Turkey*

Abstract

In this study, the changes of velocity and turbulence for an inclined jet in cross-flow are investigated experimentally. Cylindrical and rectangular hole geometries are used in the experiments. The blowing ratio is 1.75, and the injection angle with respect to the horizontal plane is 30º. The injection holes in the models are in a single row. The diameters of holes, which have a cylindrical cross section, are 8.5 mm. The rectangular cross section holes are 9 x 6.5 mm. The injection holes are inclined at 30º along the mainstream direction. The air is injected at 57 ºC and its blowing ratio is 1.75. The results show that turbulence intensity changes with hole geometry. In this study, turbulence intensity is higher in the region close to the wall because of the jet impact. The penetrations of the cylindrical jets into the main flow are deeper than the penetrations of the rectangular jets, and turbulence intensities of the cylindrical jets are larger than the penetrations of the rectangular jets.

1. INTRODUCTION

Cross-flow in jet flows, or cross jets, can be observed in several areas: Vertical take-off and landing of aircraft (in aviation), environment (confluence of rivers to the sea), and industrial applications (cooling of gas turbines, confluence of smoke released into the atmosphere). The vortex structures seen in a jet in a cross-flow phenomenon have numerous applications and are obtained using the Reynolds Stress Turbulence Model [1].

Hydrodynamic measurements of jets in cross-flow for gas turbine film cooling applications were investigated [2].

Mixing processes in turbulent fluid motion are of fundamental value in many situations in engineering practice, such as pollutant formation, heat and mass transfer, and chemical reactions. The large eddy simulation (LES) methodology was used to investigate how turbulent mixing can be enhanced by varying the angle between the jet and the oncoming cross-flow [3].

Numerical simulation of gas-solid flow was performed with an inclined jet, in a two-dimensional fluidized bed. The mechanism of jet formation was analyzed using both numerical simulations and experiments. The influences of jet velocity, nozzle diameter, nozzle inclination and jet position on jet penetration length were obtained [4].

A three-dimensional numerical simulation of fluid flow and heat transfer characteristics of an inclined jet, with cross-flow impinging on a heating plate, was presented [5]. The turbulent-governing equations are solved by a control-volume-based finite-difference method with a power-law scheme, and the well-known k–ε turbulence model and its associate wall function are used to describe the turbulent structure. The velocity and pressure terms of momentum equations are solved by the SIMPLE method.

The reactants are generally injected into industrial furnaces by jets. An effective method to act on combustion in such systems is to control the injection jets. The control of turbulent flames by the deflection of jets in a natural gas–oxygen burner was studied[6]. Results show that control by inclined jets has a considerable effect on dynamics and flame topology. Measurements showed that the deflection favors the mixing and accelerates the fusion of jets, allowing flame stabilization.

---

*Corresponding author, e-mail: ibkoc@gelisim.edu.tr

To improve the efficiency of gas turbine engines, the gas inlet temperature has to increase beyond the failure temperature of the turbine blade and vane material. In other words, gas turbine blades have to be protected from the hot gases using a thin fluid film wrapped around the blade. To achieve such a protective layer, cooler air is injected through discrete holes on the blade surface. This problem has been analyzed in several numerical and experimental studies [7-10]. The turbulent flow structure and vortex dynamics of a jet-in-a-cross-flow (JICF) problem, which are related to gas turbine blade film cooling, are investigated using the particle-image velocimetry (PIV) technique [11]. The results show a higher mass-flux ratio to enlarge the size of the recirculation region, leading to a more pronounced entrainment of hot outer fluid into the wake of the jet. The results of the experimental measurements are used to validate the numerical findings. This comparison shows an excellent agreement for mean velocity and higher moment velocity distributions.

The flow field of a radial wall jet, created by the impingement of a round synthetic jet normal to a flat surface, was characterized using hot-wire anemometry [12]. The width of the outer layer of the synthetic wall jets is observed to increase linearly with radial distance along the wall.

In this study, the changes of velocity and turbulence for an inclined jet in cross flow are investigated experimentally. Cylindrical and rectangular hole geometries are used in the experiments. The effects of the hole geometries on turbulence and velocity are compared. In addition, the penetration effects to the main flow of inclined jets are investigated.

2. EXPERIMENTAL APPARATUS AND PROCEDURE

A schematic view of the wind tunnel used in the velocity and turbulence experiments is presented in figure 2.1. The test setup consists of a fan, a heater, an orifice, a plenum chamber, a plexiglas plate, a hot-wire anemometry, a miniature wire probe (55P15), probe support for single-sensor probe, a traverse system, and a computer. The test section is 460 mm wide, 460 mm high and 610 mm long. The blowing ratio is 1.75, and the injection angle with respect to the horizontal plane is 30°.
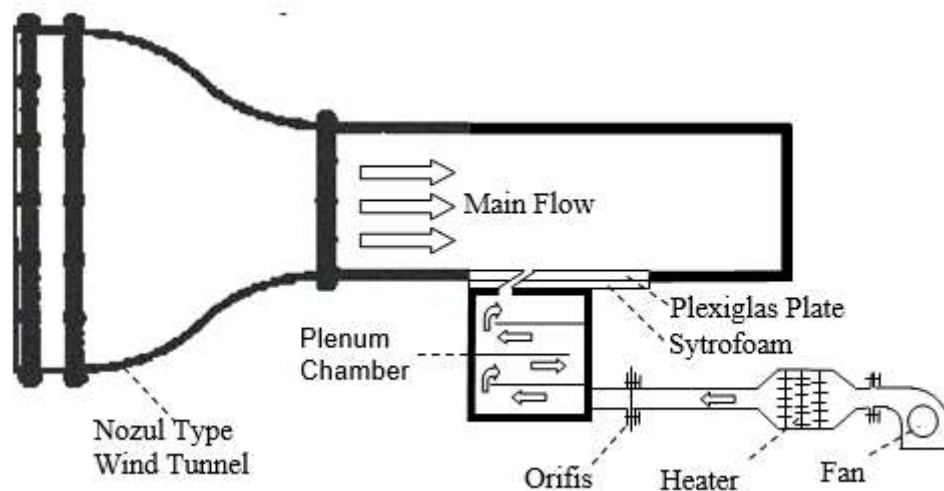

Figure 2.1. *Schematic view of the test facility*

In the experiment, a transparent plexiglas plate with a small conduction coefficient is used. A plenum chamber is used to supply a steady injection. The orifice made of plexiglas was designed to measure the flow rate of injected air. The centrifugal fan for injection of air out to the test chamber, the heater for raising the ambient temperature to 330 K, and a rheostat to control the power of heater are used. The heater has two resistances of 1000 W. The oblique manometer for calculating the mass flux of injected air, and the insulation material, which is 5 mms thick to prevent heat loss from the plexiglas surface, are used.

Hot-wire anemometry for the measurement of velocity and turbulence level in a single dimension, or a Constant-Temperature Anemometer (CTA), is used. The miniature wire probe with offset prongs and

a sensor perpendicular to the probe axis are used for velocity and turbulence measurements. This probe is designed for boundary layers. The shape of the prongs permits measurements close to a solid wall without disturbance from the probe body outside the boundary layer. Mounts with the probe axis are parallel to the direction of flow. The measurement probe is calibrated in the wind tunnel before velocity and turbulence are measured. The velocity values for calibration were 0, 5, 10, 15, 20, 25 and 30 m/s. The traverse system is used to move the probe to a known point. The computer is used to analyze the data obtained from hot wire anemometry.

In the experiment, the warmer air from the main flow is injected into the wind tunnel at 30 degrees. The main flow velocity is measured using hot wire probe. The velocity value of the fluid injected from the holes was calculated using the orifice. After the calibration, velocity and turbulence in the directions indicated in figure 2.2 are measured.
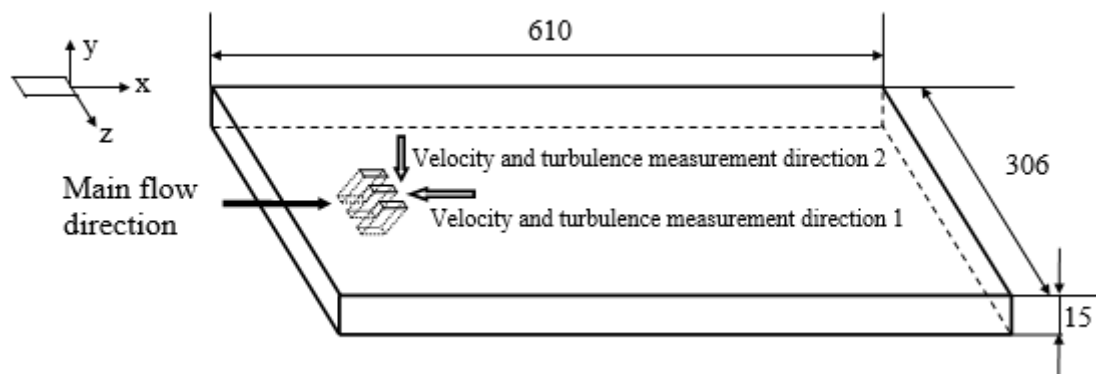

Figure 2.2 *Schematic view of the direction of velocity and turbulence measurements*

The measurement probe is positioned at the specified coordinates using the traverse system. In the experiment, the fan, heater, rheostat, and wind tunnel is run. After establishing the required conditions, the velocity and turbulence data are collected by the hot wire anemometry computationally. Measurements are made in both directions and for all the previously determined coordinate points, both for cylindrical holes and rectangular holes. The air is injected at 57°C and with a blowing ratio is 1.75. The injection velocity is used for the calculation of blowing ratio. The velocity value was found by using the orifice. The data used in the measurements are given in Table 2.1.

Table 2.1. *Values for velocity and turbulence measurements*

Hole geometry	Injected air characteristics				Main flow characteristics				
	T_j(K)	V_j(m/s)	ρ_j(kg/m³)	$\dot{m}$(kg/s)	T_∞(K)	V_∞(m/s)	ρ_∞(kg/m³)	M	I
Cylindrical	330	21.60	1.0516	0.0143	300.0	10.800	1.1774	1.75	3.57
Rectangular	330	18.19	1.0516	0.0140	302.0	9.600	1.1703	1.75	3.23

Measurements were made for cylindrical holes after the sixth hole. The diameters of the holes with a cylindrical cross section are 8.5 mm. Eleven injection holes on the model are in a single row. The schematic view of cylindrical holes is presented in figure 2.3. Coordinate axes are positioned as out from the sixth hole.
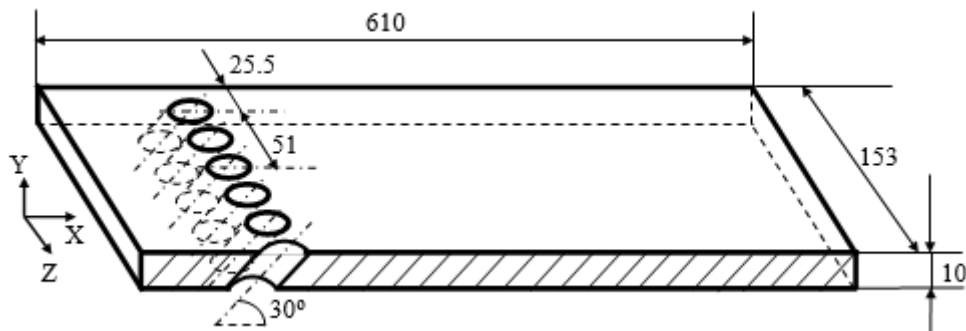
Figure 2.3. Schematic view of cylindrical holes

Three injection holes are located on a plexiglas plate. The holes are 9 x 6.5 mm. All hole geometries in the model are rectangular and with the same cross-section area. The injection angles are 30° to the surface and the main flow. Measurements were made for a single row at the second hole. The schematic view of the rectangular holes is presented in figure 2.4.
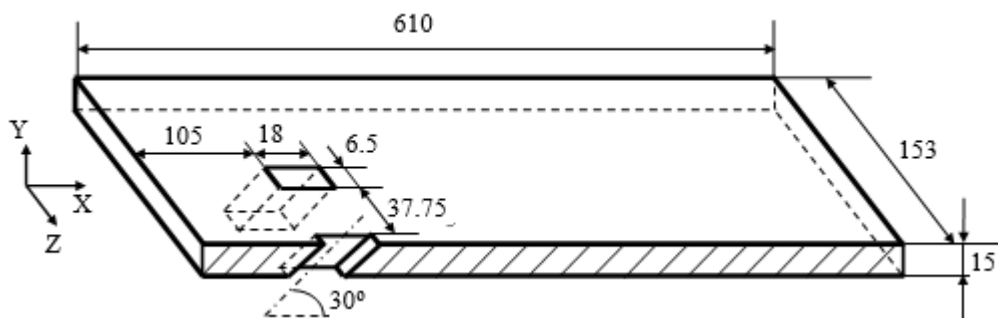

Figure 2.4. Schematic view of the rectangular holes

The measurement points of probe for the measurements of velocity and turbulence are given in Table 2.2.

Table 2.2. Values for velocity and turbulence measurements

X/D_1	X/D_2	Z/D_1	Z/D_2	Y(mm)
	-1			1.5
	0		-1	3
	1		0	7
	2		0.5	12
	3			17
	4			22

In this table, D2 is hydraulic diameter of the rectangular film holes. It is calculated using equation 1,

$$D_2 = \frac{4A}{P} \tag{1}$$

where A is the cross-section area of the rectangular hole, and P is the wet perimeter. D_2 value is determined to be 7.55 mm for the rectangular hole.

The mainstream air velocity and the injected air velocity ratio are determined using the blowing ratio,

$$M = \left(\frac{\rho_j V_j}{\rho_\infty V_\infty} \right) \qquad (2)$$

where M is the blowing ratio, ρ_j is the injected fluid density, V_j is the injected fluid velocity, ρ_∞ is the main flow density, and V_∞ is the main flow velocity. M was determined to be 1.75. The injected fluid velocities (V_j) were calculated using (2).

One of the parameters that affect the flow field is the momentum flux ratio. The momentum flux ratio is used as physical justification for choosing the blowing ratio. It is well accepted that the key parameter of jet penetration in a cross-flow is the momentum flux ratio, shown in equation 3. In the experiment, the different momentum fluxes are obtained by changing the temperature of the injected air. The momentum flux ratio is determined by Goldstein et al. [13] as follows:

$$I = \frac{\rho_j V_j^2}{\rho_\infty V_\infty^2} \qquad (3)$$

where I is the momentum flux ratio. The momentum flux ratio values are given in table 1.

The turbulence intensity is determined by Kunda and Cohen [14] as follows:

$$Tu = \frac{u'}{\overline{V}} \qquad (4)$$

$$u' = \sqrt{\overline{u^2}} \qquad (4a)$$

where T_u is turbulence intensity, $\overline{V}$ is mean velocity and   is the root-mean-square of the turbulent velocity fluctuations. For experimental studies, uncertainty analysis is presented. The error is calculated using the following equation [15]:

$$w_R = \left[\left(\frac{\partial R}{\partial X_1} w_1 \right)^2 + \left(\frac{\partial R}{\partial X_2} w_2 \right)^2 + ... + \left(\frac{\partial R}{\partial X_n} w_n \right)^2 \right]^{1/2} \qquad (5)$$

where R is the magnitude measured in the system, X is the independent variable and w is the error rate of the independent variable.

Error percentages obtained from the uncertainty analysis are given in table 2.3.

Table 2.3. *Error percentages obtained from the uncertainty analysis*

Hole geometry	% Uncertainty								
	T_j	V_j	ρ_j	$\dot{m}$	T_∞	V_∞	ρ_∞	M	I
Cylindrical	0.05	6.79	2	6.42	0.05	1	0.05	7.05	13.87
Rectangular									

3. RESULTS AND DISCUSSION

In the main flow direction, velocity profiles obtained for a cylindrical hole are given in figure 3.1. As seen in the figure, the velocity decreases in the main flow direction. However, the Y position of the maximum velocity increases. For example, the velocity is maximum at z* = 0, X = 0 and Y = 3 mm at a value of 27.68 m/s. The lateral direction is shown as z*, where z* = Z/D$_1$ is the characteristic length (D$_1$ = 8.5 mm is used for this study). However, the maximum velocity is 17.70 m/s at z* = 0,

X = 34 mm and Y = 17 mm. In addition, significant changes are observed in the direction of the main flow velocities close to the hole.
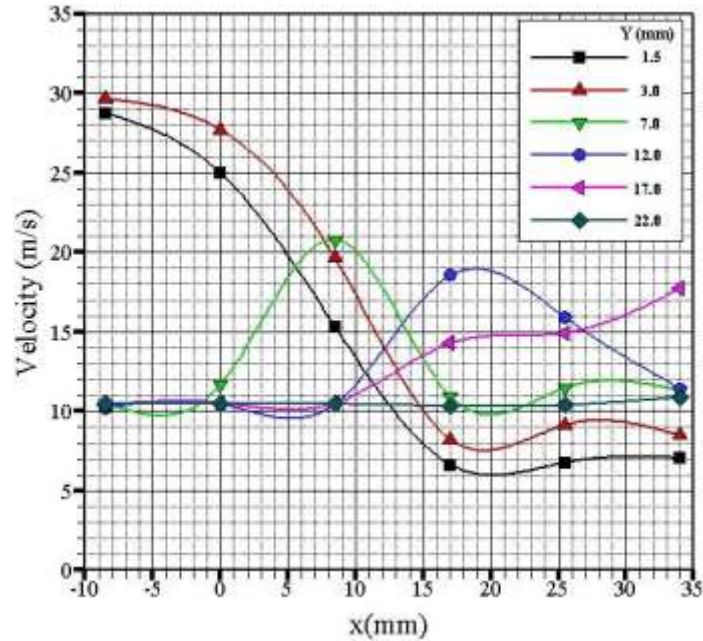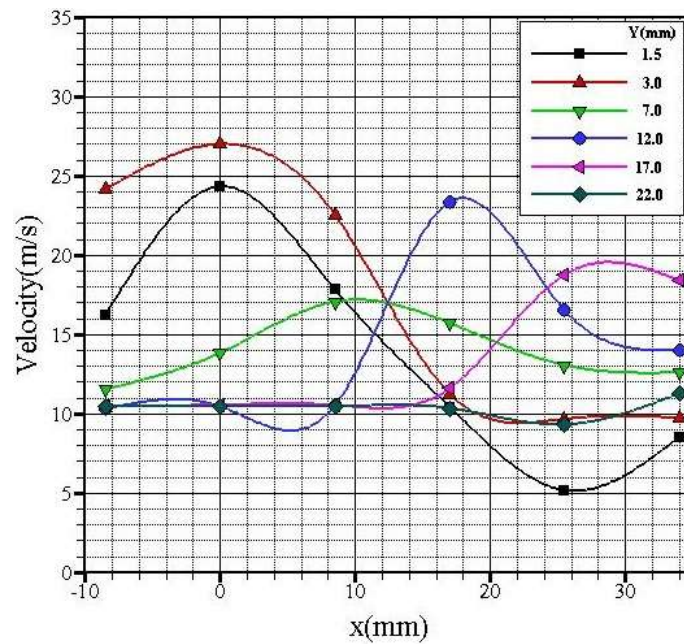

Figure 3.1. *Velocity profiles in the main flow direction for a cylindrical hole($z^* = 0$)*

In the main flow direction, velocity profiles obtained for a cylindrical hole at $z^* = 0$ are given in Figure 3.2. As seen in the figure, the velocity decreases in the Y direction. However, the Y position of the maximum velocity increases. For example, the velocity is maximum at $z^* = -1$, X = 0 and Y = 3 mm at a value of 11.30 m/s. However, the maximum velocity is 11.59 m/s at $z^* = -1$, X = 17 mm and Y = 7 mm. If y is increased, the flow becomes more stable, and the flow jet is more flexible.
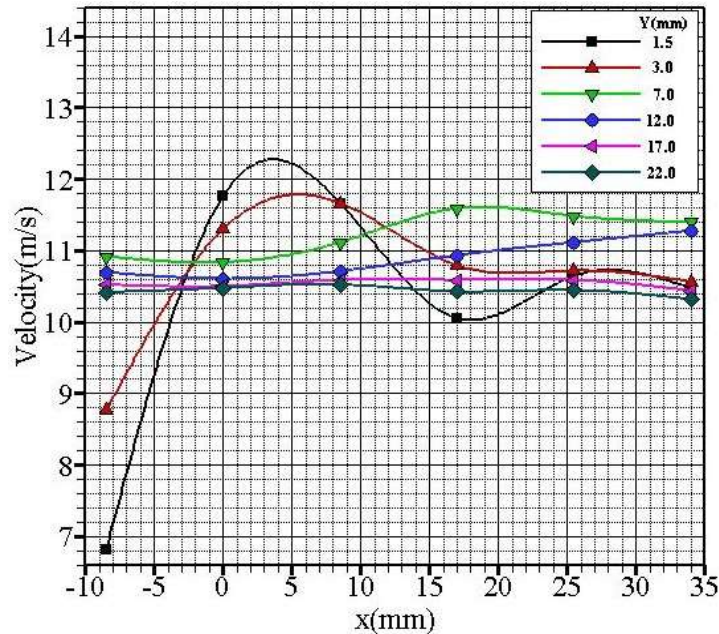
Figure 3.2. *The velocity profiles in the main flow direction for a cylindrical hole($z^* = -1$)*

Harmonic motion in jet velocity is observed in the main flow direction when the inclined jet is bent by hitting the wall . In the main flow direction, velocity profiles obtained for a cylindrical hole at $z^* = 0.5$ are given in Figure 3.3.
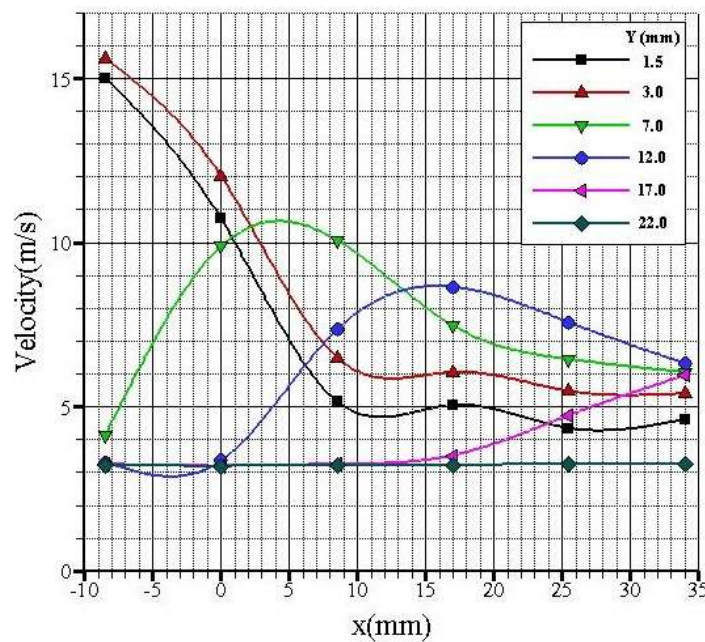
Figure 3.3. *The velocity profiles in the main flow direction for a cylindrical hole(z* = 0.5)*

In Y direction, velocity profiles obtained for a cylindrical hole at $z^* = 0$ are given in Figure 3.4. As seen in the figure, the velocity decreases in the Y direction. The maximum value of the velocity component in the Y direction varies with the direction of the main flow. For example, the velocity is maximum at $X = 0$ and $Y = 3$ mm and its value is 12.02 m/s. The velocity is maximum at $X = 0$ and $Y = 7$ mm and its value is 10.07 m/s. The velocity is maximum at $X = 0$ and $Y = 12$ mm and its value is 8.6 m/s.

Figure 3.4. *The velocity profiles in Y direction for a cylindrical hole(z* = 0)*

In the Y direction, velocity profiles obtained for a cylindrical hole at $z^* = -1$ and $z^* = 0.5$ are given respectively in Figure 3.5 and Figure 3.6. Figure 3.5 and Figure 3.6 show characteristics similar to Figure 3.4.
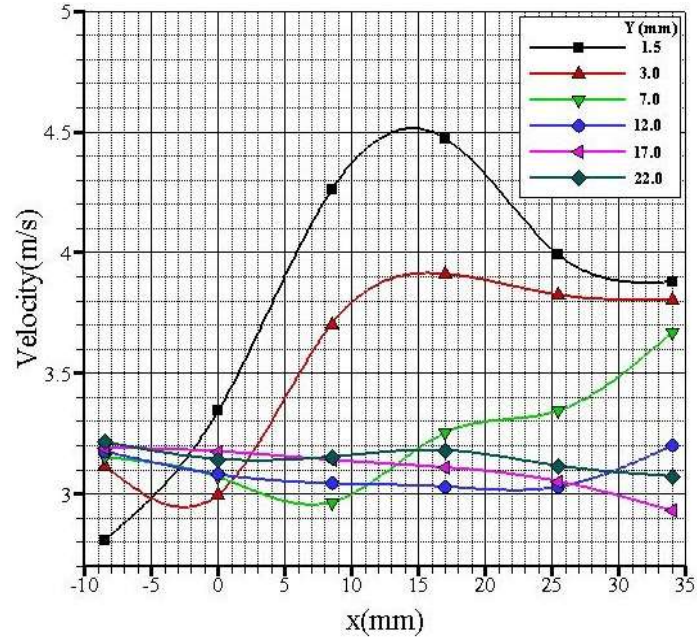
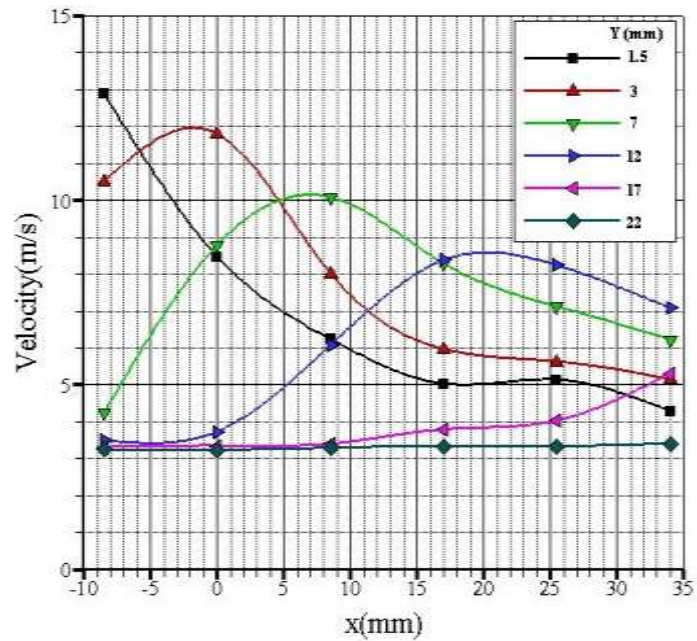**Figure 3.5.** *Velocity profiles in Y direction for a cylindrical hole(z* = -1)*

Figure 3.6. *Velocity profiles in Y direction for a cylindrical hole(z* = 0.5)*

In the main flow direction, the turbulence measurements obtained for a cylindrical hole are given in figure 3.7-3.9. In the figures, the maximum turbulence value is 34.97% for $z^* = 0$, 45.19% for $z^* = 0.5$, and 10.83% for $z^* = -1$. The turbulence intensity outside the mixing zone ranges from 1.10% to 1.75%. Turbulence intensity is higher in the region close to the wall.
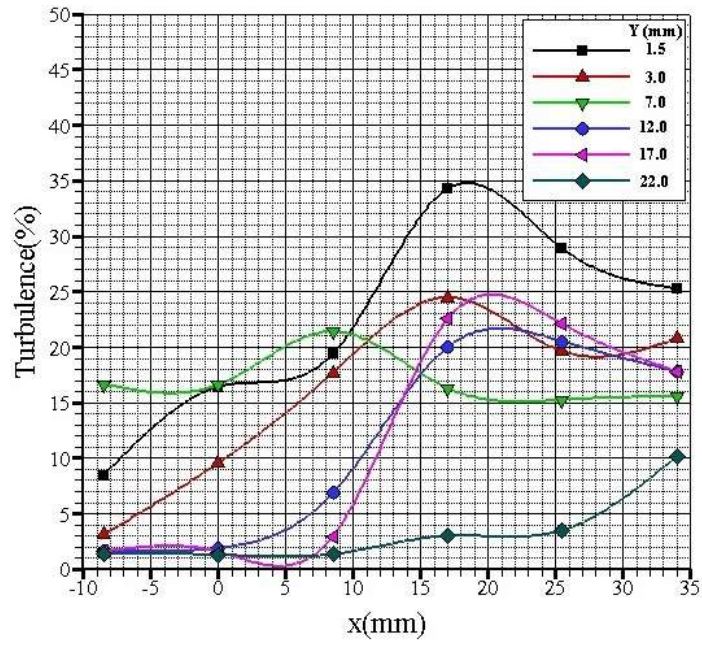
Figure 3.7. Turbulence intensity in the main flow direction for a cylindrical hole($z^* = 0$)
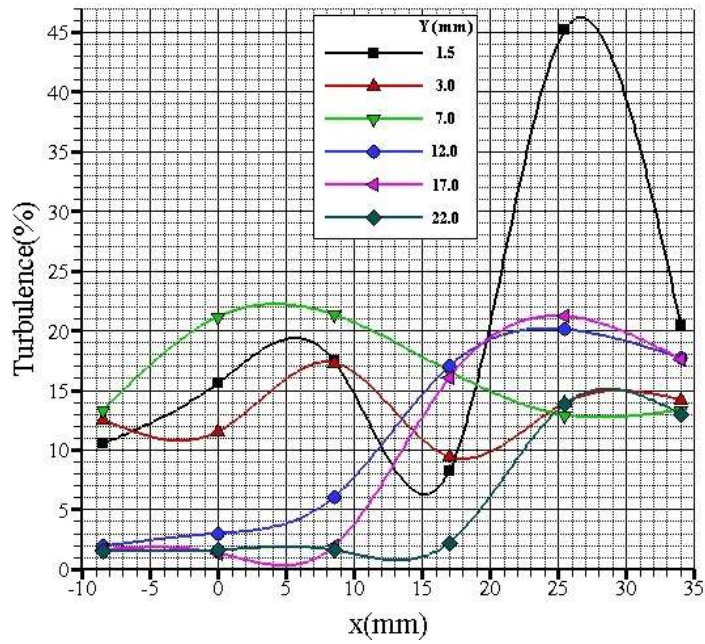

Figure 3.8. Turbulence intensity in the main flow direction for a cylindrical hole($z^* = 0.5$)
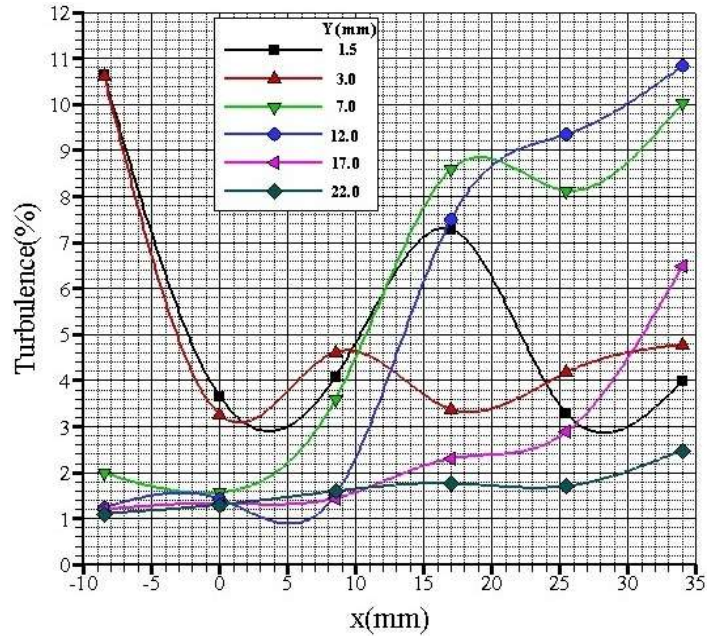
Figure 3.9. *Turbulence intensity in the main flow direction for a cylindrical hole(z* = -1)*

In Y direction, the turbulence measurements obtained for a cylindrical hole are given in figure 3.10-3.12. The figures are examined, the maximum turbulence value is 37.29% for $z^* = 0$, 34.51% for $z^* = 0.5$, and 31.77% for $z^* = -1$. The turbulence intensity outside the mixing zone ranges from 4.9% to 5.7%. The maximum turbulence intensity values in the main flow and Y direction are compared and the greater turbulence intensity values are determined in the Y direction.
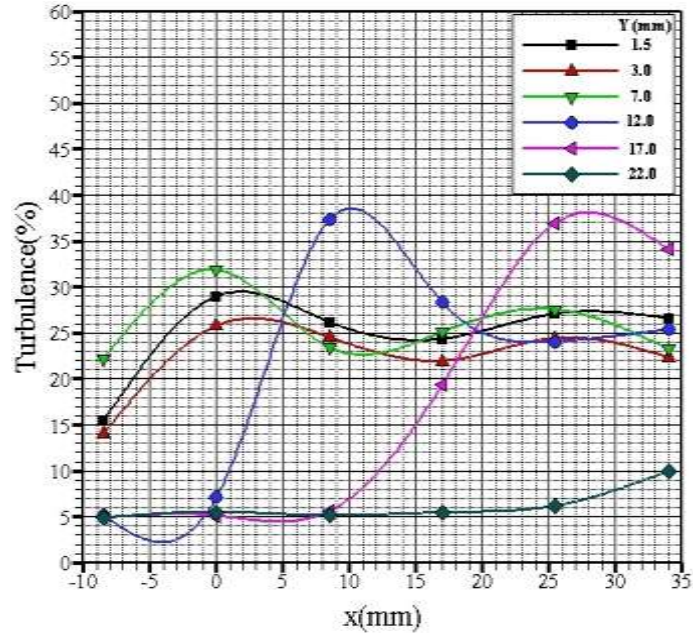

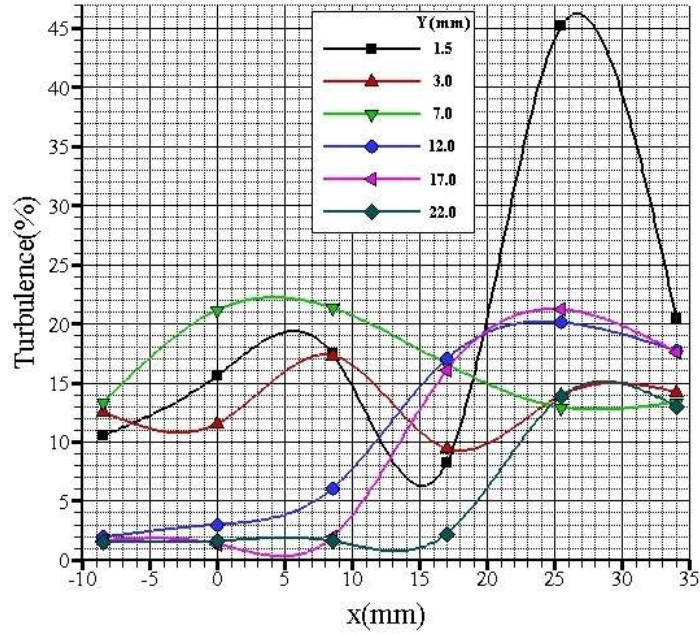***Figure 3.10.*** *Turbulence intensity in Y direction for a cylindrical hole (z* = 0)*

Figure 3.11. *Turbulence intensity in Y direction for a cylindrical hole (z* = 0.5)*
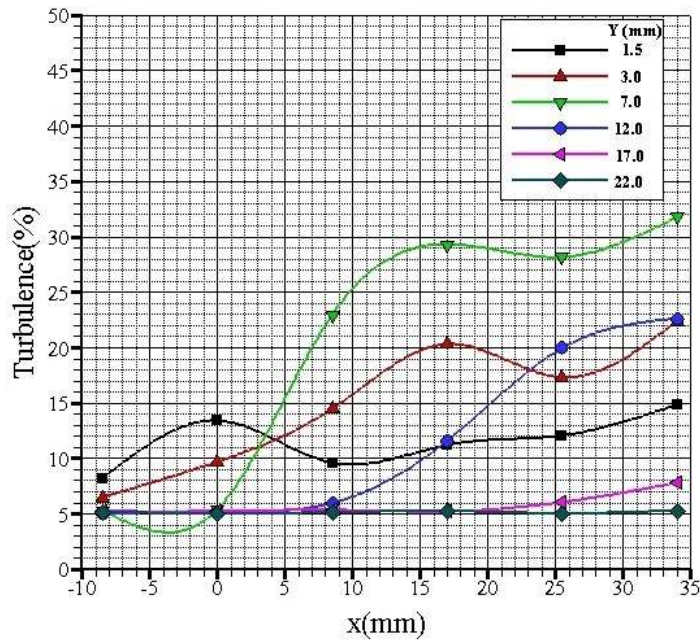

Figure 3.12. *Turbulence intensity in Y direction for a cylindrical hole (z* = -1)*

In the main flow direction, velocity profiles obtained for a rectangular hole are given in Figures 3.13-3.14. The measured velocities in the main flow direction for a rectangular hole are examined, and the velocity decreases in the main flow direction. A harmonic motion in jet velocity is observed in the main flow direction when the inclined jet is bent by hitting the wall. The main flow velocity value is approximately 9.8 m/s. The lateral direction is shown with z*, where $z^* = Z/D_2$ is the characteristic length ($D_2 = 7.55$ mm is used for this study).
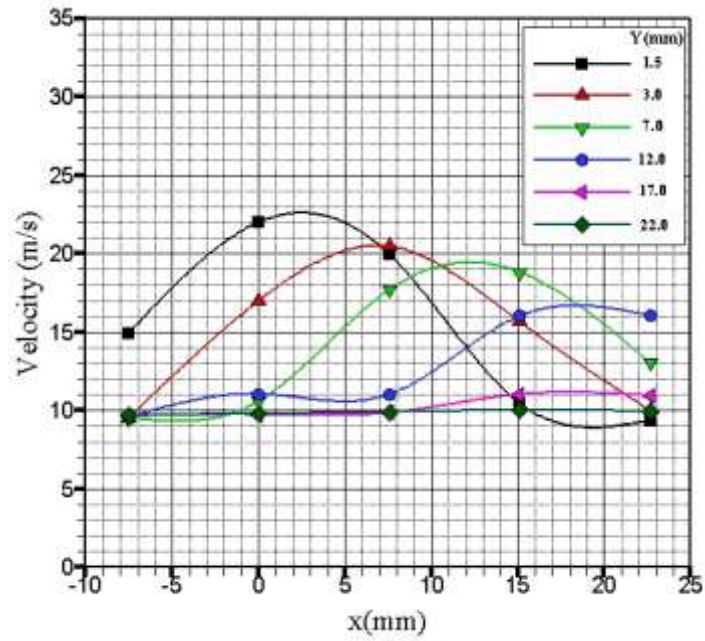
Figure 3.13. *Velocity profiles in the main flow direction for a rectangular hole (z* = 0)*
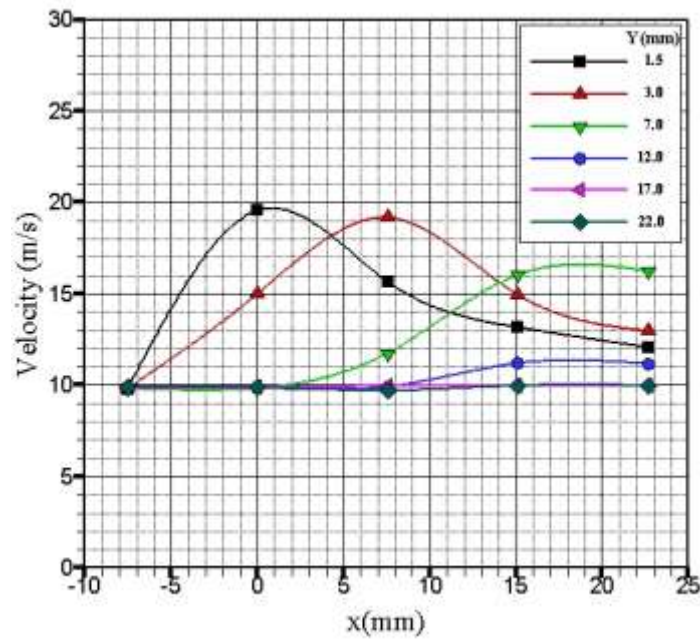

Figure 3.14. *Velocity profiles in the main flow direction for a rectangular hole (z* = 0.5)*

In the main flow direction, the turbulence measurements obtained for a rectangular hole as a single row are given in Figures 3.15-3.16. In the figures, the maximum turbulence value is 24.01% for $z^* = 0$, and 19.38% for $z^* = 0.5$. The turbulence intensity outside the mixing zone ranges from 2.98% to 3.10%.
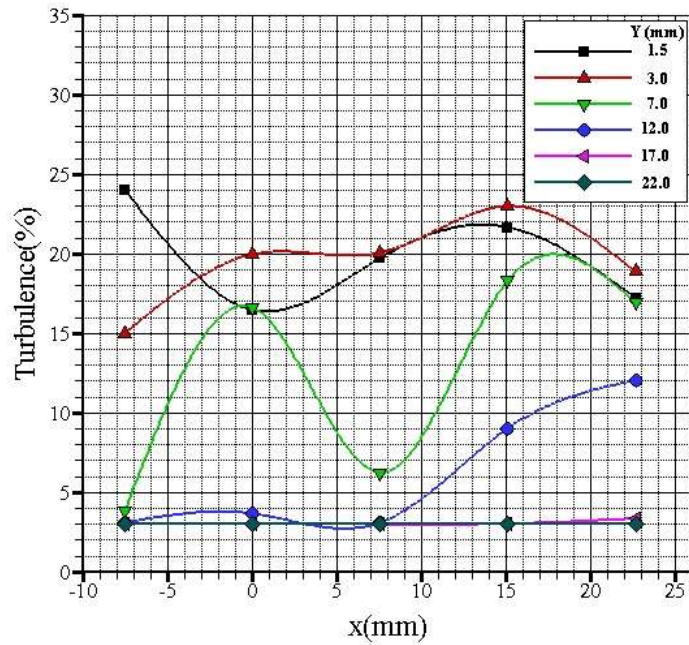
Figure 3.15. *Turbulence intensity in the main flow direction for a rectangular hole (z* = 0)*
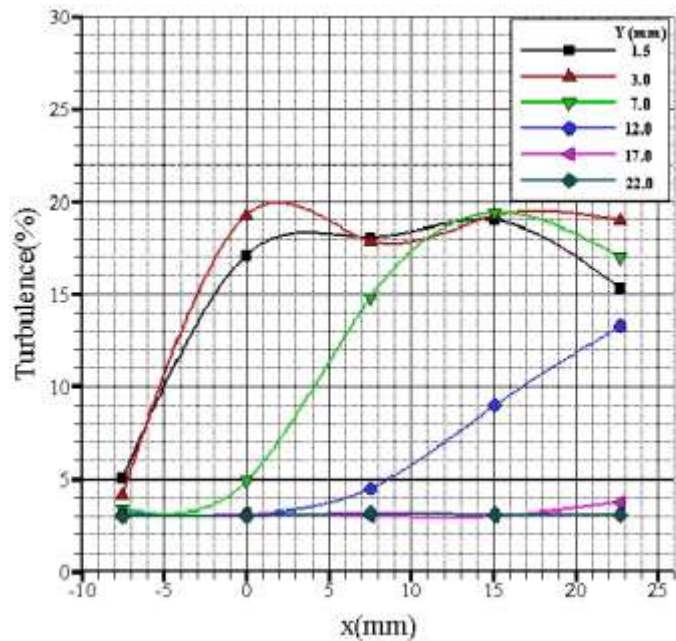

Figure 3.16. *Turbulence intensity in the main flow direction for a rectangular hole (z* = 0.5)*

4. CONCLUSION

In this study, the changes of velocity and turbulence for an inclined jet in cross flow are investigated experimentally. Cylindrical and rectangular hole geometries are used in the experiments. The results show that the main flow velocity is reduced in X direction.

Turbulence intensity changes with hole geometry.

Turbulence intensity is higher in the region close to the wall because of jet impact.

The penetration of the cylindrical jets into the main flow is deeper than the penetration of the rectangular jets.

Turbulence intensity decreases away from the jet holes.

Turbulence intensity of cylindrical jets is larger than that of rectangular jets.

NOMENCLATURE

A   Cross-section area [mm^2]

I   Momentum flux ratio [–]

M   Blowing ratio [–]

$\dot{m}$ Mass flow rate [kg/s]

P   Wet perimeter   [mm]

T_u Turbulence intensity

T_j Injection fluid temperature [K]

T_∞ Main flow temperature [K]

$u^{'}$ The root-mean-square of the turbulent velocity fluctuations [m/s]

$\overline{V}$ Mean velocity [m/s]

V_j Injection fluid velocity [m/s]

V_∞ Main flow velocity [m/s]

x   Length in mainstream direction [mm]

z   Length in lateral direction [mm]

ρ_∞ Main flow density [kg/m^3]

ρ_j Injection fluid density [kg/m^3]

CONFLICT OF INTEREST

No conflict of interest was declared by the authors

REFERENCES

[1]   Bayraktar S. and Yilmaz T., "The Investigation of Vortices by Using Second Order Turbulence Closure", Journal of Aeronautics and Space Technologies, 3:7-15, (2007).

[2]   Pietrzyk J.R., Bogard D.G. and Crawford M.E., "Hydrodynamic Measurements of Jets in Crossflow Gas Turbine Film Cooling Applications", Journal of Turbomachinery, 111:139-145, (1989).

[3]   Wegner B., Huai Y. and Sadiki A., "Comparative Study of Turbulent Mixing in Jet in Cross-Flow Configurations Using LES", International Journal of Heat and Fluid Flow, 25:767–775, (2004).

[4]   Hong R., Li H., Ding J. and Li H., A Correlation Equation for Calculating Inclined Jet Penetration Length in a Gas-Solid Fluidized Bed, China Part, 3(5):279-285, (2005).

[5]   Yang Y-T. and Wang Y-X., "Three-Dimensional Numerical Simulation of an Inclined Jet with Cross-Flow", International Journal of Heat and Mass Transfer, 48, 4019–4027, (2005).

[6]   Boushaki T., Mergheni M.A., Sautet J.C. and Labegorre B., "Effects of Inclined Jets on Turbulent Oxy-Flame Characteristics in a Triple Jet Burner", Experimental Thermal and Fluid Science, 32, 1363–1370, (2008).

[7]   Walters D.K. and Leylek J.H., "A Detailed Analysis of Film Cooling Physics: Part I – Streamwise Injection with Cylindrical holes", Journal of Turbomachinery, 122, 102–112, (1997).

[8]   Baldauf S., Schulz A. and Wittig S., "High-Resolution Measurements of Local Effectiveness From Discrete Hole Film Cooling", Journal of Turbomachinery, 123, 758–765, (2001).

[9]   Guo X., Schröder W. and Meinke M., "Large-Eddy Simulations of Film Cooling Flows", Computer & Fluids, 35, 587–606, (2006).

[10]   Koc I., "Experimental and Numerical Investigation of Film Cooling Effectiveness for Rectangular Injection Holes", Aircraft Engineering and Aerospace Technology", 79, No.6, 621-627, (2007).

[11]   Jessen W., Schro¨der W., Klas M., "Evolution of Jets Effusing from Inclined Holes into Crossflow", International Journal of Heat and Fluid Flow, 28, 1312–1326, (2007).

[12]   Krishnan G. and Mohseni K., "An Experimental Study of a Radial Wall Jet Formed by the Normal Impingement of a Round Synthetic Jet", European Journal of Mechanics - B/Fluids, 29, 269-277, (2010).

[13]   Goldstein R.J., Eckert E.G.R. and Burggraf F., "Effects of Hole Geometry and Density on Three-Dimensional Film Cooling", International Journal of Heat and Mass Transfer, 17, 595-607, (1974).

[14]   Kunda P.K. and Cohen I.M., Fluid Mechanics, Academic Press, SanDiego, California, United States of America, (2002).

[15]   Genceli, O. F., 2000. Ölçme Tekniği, Birsen Yayınevi, Cağaloğlu, İstanbul, (2000).